行政院國家科學委員會補助專題研究計畫 ■成果報告
□期中進度報告

合成具開口碳六十及內包氫氣、氦氣與釓離子之化學反應探討

計畫類別：■個別型計畫　□整合型計畫
計畫編號：NSC98－2119－M－009－001－MY2
執行期間：99 年 08 月 01 日至 100 年 07 月 31 日

執行機構及系所：國立交通大學應用化學系

計畫主持人：莊士卿
共同主持人：
計畫參與人員：鄧桔程、林鈺偉、鄭淳安、劉正揚、范瑞杰、黃倩妤、詹富為、郭志偉

成果報告類型(依經費核定清單規定繳交)：□精簡報告　■完整報告

本計畫除繳交成果報告外，另須繳交以下出國心得報告：
□赴國外出差或研習心得報告
□赴大陸地區出差或研習心得報告
□出席國際學術會議心得報告
□國際合作研究計畫國外研究報告

處理方式：除列管計畫及下列情形者外，得立即公開查詢
■涉及專利或其他智慧財產權，□一年■二年後可公開查詢

（一） 計畫中文摘要

由於具開口碳六十之分子容器無法以傳統的電弧放電方式獲得，目前只能依賴有機合成方式。本計劃實行的重點在於以合成方法達到含氫氣、氨氣與釓金屬離子之開口碳六十為方向，以應用於儲氫、儲氨之分子容器及應用於內包釓金屬離子做為核磁共振顯影劑。此計劃第一階段將探討以有機金屬催化合成反應獲得具開口之碳六十衍生物，例如以鎳或鈀金屬催化碳六十環化反應。第二階段為探討將具有開口碳六十衍生物，以化學方法形成一個大的開口，再置入氫氣與氨氣。

關鍵詞: 碳六十、開口碳六十、分子容器、氫氣、氨氣、金屬催化

（二） 計畫英文摘要。

Organic synthesis of open-cage fullerenes and atempts to synthesize open fullerenes with hydrogen, ammonia and gadolinium inside the cage is described. The desire for these endohedral open-cage fullerenes is primarily driven from their potentialities as hydrogen or ammonia-container in the frontier material field and superior magnetic resonance imaging agent in biomedical field. The availability of these compounds has yet to rely on organic synthesis because they can not be obtained from conventional electrical arc discharge method. The described approach herein starts from metal-catalyzed cycloaddition with C_{60}. A large opening will be formed by controlled bond scissions. The synthesized open-cage fullerenes can be molecular containers that will be inserted hydrogen or ammonia at high pressure.

Keyword: C_{60}, open-cage fullerene, molecular container, hydrogen, ammonia, metal-catalysis

（二）報告內容

Introduction

Fullerene materials remain one of the good candidate materials for resolving issues with energy. Fullerenes can be modified chemically to form an opening and subsequently inserted with guest molecules as hydrogen. Insertion of other large guest molecules as ammonia or methane could be possible. The desire for larger opening on fullerenes remains highly demanded for study of encapsulation of larger species. In the first term of this project, we investigate metal-catalyzed functionalization for derivatizing C_{60} for future opening on C_{60} through synthetic approach by merging two chemically-opened holes**.**

Results and discussion

In the first period of this project, we have found a palladium-catalyzed annulation of benzamides with C_{60}. First, we synthesized the N-alkylated benzamides **1a**–**j** according to conventional methods. We used *N*-methylbenzamide (**1a**) as a standard substrate for our optimization studies. Initially, we evaluated the reaction of C_{60} (36 mg, 0.050 mmol) with **1a** (20 mg, 0.15 mmol) in the presence of $Pd(OAc)_2$ (1.1 mg, 0.0050 mmol, 10%) and oxone (22 mg, 0.15 mmol) in *o*-DCB/TFA (6:1, v/v; 7 mL) at 120 °C in a sealed tube for 24 h; we obtained the desired C_{60}-fused isoquinolinone **2a** in 33% isolated yield, 45% based on recovered C_{60} (Table 1, entry 1). Although the formation of this fulleroisoquinolinone was relatively efficient under these conditions, we explored reactions using other oxidizing agents and solvents in a quest for better yields. The corresponding reactions performed using the common oxidants $Cu(OAc)_2$, CH_3COOAg,[1] and Ag_2O,[2] under the standard conditions described above, improved the yields of **2a** to 50, 45, and 38%, respectively (Table 1, entries 3–5). Next, we tested the catalytic reaction using AcOH,[3] DMSO,[4] CH_3CN,[5] and 1-chloronaphthalene as co-solvents, but the resulting transformations were relatively less efficient (entries 6–10). The reactions performed in chlorobenzene/TFA (10:1) gave **2a** in 42% yield with only a trace amount of recovered C_{60} (entry 11). The addition of one equiv. of water deteriorated the reaction performance (entry 12).

Table 1. Reactions of C_{60} with **1a** Under Various Conditions

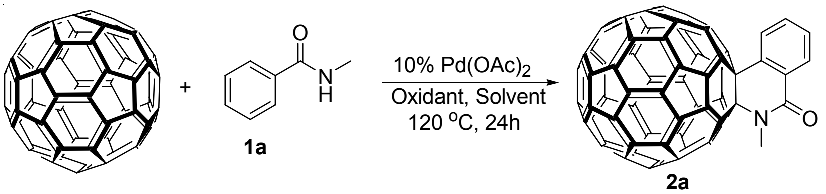

entry	oxidant	solvents (mL)	Yield (%)
1	Oxone	*o*-DCB/TFA (6:1)	33 (45)
2	Oxone	*o*-DCB/DMSO(6:1)	7 (32)
3	$Cu(OAc)_2$	*o*-DCB/TFA (6:1)	50 (84)
4	CH_3COOAg	*o*-DCB/TFA (6:1)	45 (85)
5	Ag_2O	*o*-DCB/TFA (6:1)	38 (53)
6	$Cu(OAc)_2$	*o*-DCB/AcOH (6:1)	4 (10)
7	Cu(OAc)	*o*-DCB/DMSO (6:1)	<3
8	$Cu(OAc)_2$	*o*-DCB/CH_3CN (6:1)	<3
9	CH_3COOAg	*o*-DCB/AcOH (6:1)	5 (12)
10	$Cu(OAc)_2$	1-Cl-naphthalene/TFA (6:1)	14 (86)
11	$Cu(OAc)_2$	PhCl/TFA(10:1)	42
12	$Cu(OAc)_2$	*o*-DCB/TFA (6:1)	37 (55)

We further evaluated the catalytic scope of this system by employing a variety of substrates **1b**–**j** (Table 2) featuring either electron-donating and -withdrawing groups on their benzamide aryl ring. In general, substrates equipped with electron-donating groups afforded their corresponding fulleroisoquinolinones in good yields (Table 2, entries 4–7). Substrates **1e** and **1f** underwent regioselective C–H activations[7] at their less-hindered and more-electron-rich para positions (relative to their Me substituents) to afford **2e** and **2f** in excellent yields of 63 and 61%, respectively (Table 2, entries 5 and 6). Substrates bearing electron-withdrawing groups, such as the chloro and phenyl units of **1h**–**j**, provided their products in only moderate yields (Table 2, entries 8–10). Under the standard conditions, the reactions of amides bearing N-benzyl substituents (**1c**, **1d**, **1g**, **1j**) yielded debenzylated products. To overcome this problem, we performed these experiments using only 0.2 mL of TFA, obtaining the desired products in moderate yields (Table 2, entries 3, 4, 7, and 10).

Table 2. Palladium-Catalyzed Syntheses of the Fulleroisoquinolinones **2a**–**j**

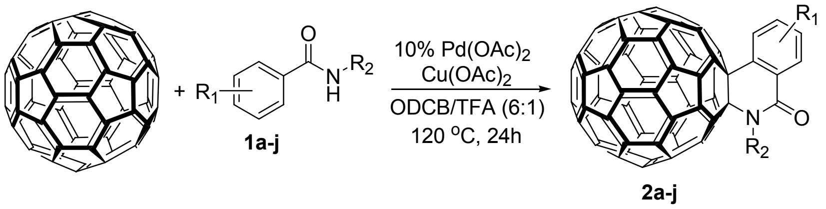

entry	amide **1**	product	yield (%)	recovered C_{60} (%)
1	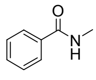	**2a**	50 (84)	42

2	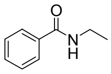	**2b**	72 (78)	8
3	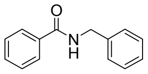	**2c**	30 (39)	22
4	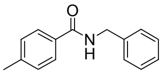	**2d**	34 (62)	44
5	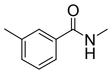	**2e**	63	trace
6	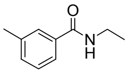	**2f**	61 (84)	28
7[c]	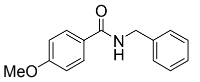	**2g**	40 (76)	47
8	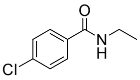	**2h**	31 (56)	44
9	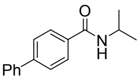	**2i**	20 (48)	55
10	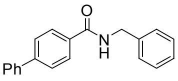	**2j**	24 (41)	42

We characterized the fulleroisoquinolinones **2a–j** using infrared (IR) and ^{1}H and ^{13}C nuclear magnetic resonance (NMR) spectroscopy, fast atom bombardment mass spectrometry (FAB MS), and X-ray crystallography. Figure 1 presents the structure of compound **2d** determined using X-ray diffraction analysis. we have achieved metal-catalyzed functionalization in the first step, our next goal will be extending this type of molecule toward opening. The following work is under progress using debenzylated compounds.

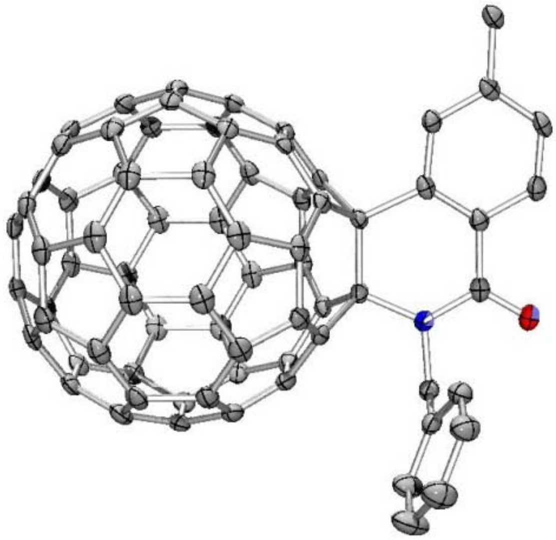

Figure 1. X-ray crystal structure of compound **2d**.

In another approach, we used conventional organic approach to prepare open-cage fullerenes for storage of hydrogen and ammonia, and also attempt to insert metallic species to the cavity of the open fullerenes. The following scheme described our methods for the preparation of these different sizable open-cage fullerenes. First, we efficiently prepared open-cage fullerenes **6** starting with [4+2] cycloaddition of diazene **5** with C_{60} in 1-chloronaphthalene at 270 ^{o}C (scheme 1). The diazene **5** was synthesized by inverse-electron demand Diels-Alder reaction of bis(2-thienyl)tetrazine (**3**) with hept-6-enoic acid ethyl ester (**4**) followed by oxidation. Open-cage fullerenes **7a-b**, derivatized from **6** by O_2 oxidation featuring a 12-membered-ring opening, consisted of isomeric structures of **7a**/**7b** in 60/40 molar ratio by ^{1}H NMR analyses. Derivatives **8a-b**, **9a-b** and **10a-b**[6], with 13, 16 and 20-membered-ring orifices respectively, were prepared through reaction of a mixture of **7a-b** with sulfur/TDAE, hydrazine/pyridine and *o*-phenylenediamine/pyridine by carbon-carbon bond scissions; their isomeric molar ratios, in 60/40, 57/43 and 51/49 respectively, were determined by ^{1}H NMR spectroscopy.[7] These open-cage fullerenes were characterized using infrared (IR) and ^{1}H nuclear magnetic resonance (NMR) spectroscopy, and MALDI-TOF mass spectrometry.[8] The isolated compounds are soluble in CS_2, $CHCl_3$, and *o*-dichlorobenzene (*o*-DCB); compounds **9a**-**b** are relatively lower in solubility than compounds **6, 7a-b, 8a-b,** and **10a-b** in these solvents.

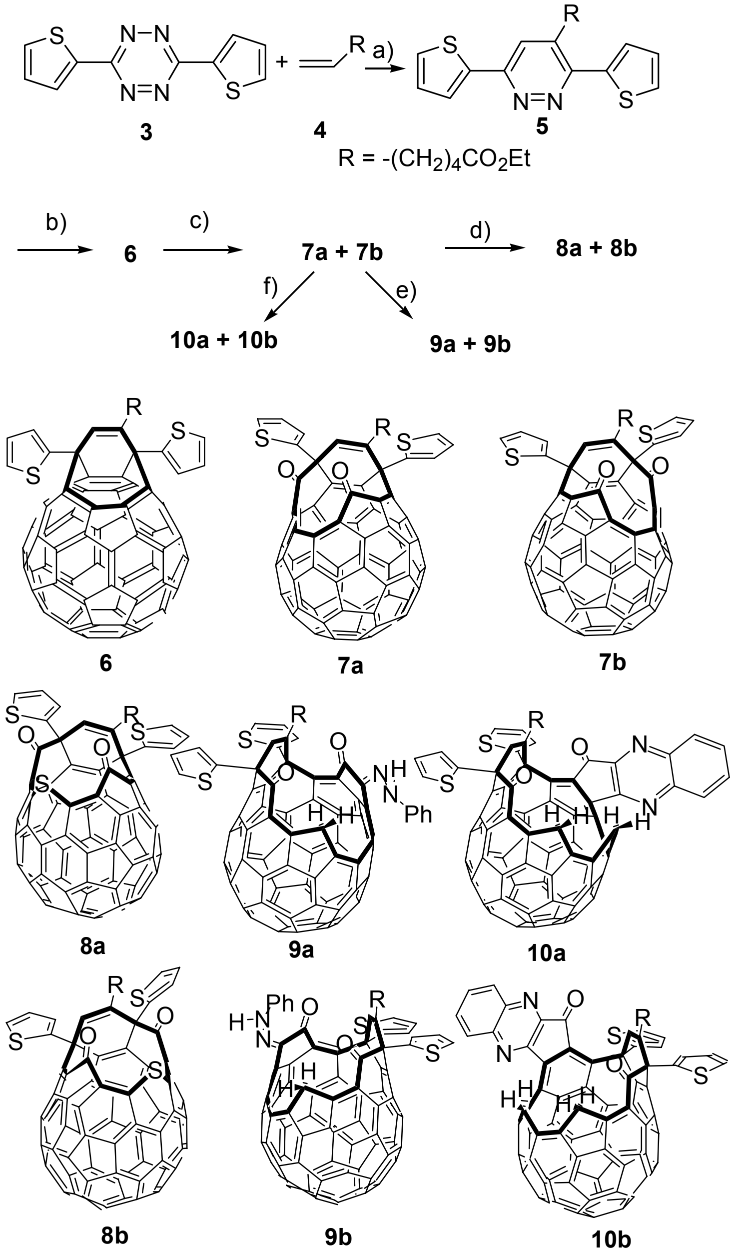

Scheme 1. Synthesis of open-cage fullerenes **6**, **7a-b**, **8a-b**, **9a-b** and **10a-b**. Conditions a) *o*-xylene, 140 ^{o}C, 24h (in pressured tube); then bubbling O_2 for 15 min; *o*-xylene, 140 ^{o}C, 24h again (39%); b) 1-chloronaphthalene, reflux, 48h (39%; 85% based on converted C_{60}); c) O_2, CS_2, $h\nu$, 3h (67%); d) tetrakis(dimethylamino)ethene (TDAE), *o*-DCB, 180 ^{o}C, 10 min (91%); e) phenylhydrazine, pyridine, *o*-DCB, 65 ^{o}C, 2h (49%); f) *o*-phenylenediamine, pyridine, *o*-DCB, 65 ^{o}C, 18h (69%).

We used cyclic voltammetry (CV, Fig. 2) to examine the redox properties of **6**, **7a-b**, **8a-b**, **9a-b** and **10a-b.** Table 1 lists the half-wave reduction potentials relative to ferrocene/ferrocenium, LUMO energy level, band gap, HOMO energy level of these studies compounds. We found that compound **7a-b**, with its lower LUMO energy level at –3.97 eV, are exceptionally easier to be reduced than all the other open-cage compounds likely due to the joint enone moieties; the observed LUMO energy levels descend in the order of **9a-b** > **6** > **PC$_{61}$BM** > **8a-b** > **10a-b** >

7a-b. Due to the lower LUMO energy level, compound **7a-b** are rather reactive toward nucleophiles; consequently, compound **8a-b**, **9a-b** and **10a-b,** derivatized from **7a-b**, possess higher LUMO energy levels for lack of combined enones moieties. Fig. 3 shows the energy level diagram determined from the onset potential of the first reductions and UV-vis spectra for all compounds. The bandgaps of **7a-b**, **9a-b** and **10a-b** are relatively smaller than those of **PC$_{61}$BM**, **6** and **8a-b**. According to these results, we would expect that **9a-b** exhibit the largest open-circuit voltage (V_{oc}) with P3HT in the device among the studied compounds. The V_{oc} is determined by the difference of the HOMO energy level of P3HT to the LUMO energy level of open-cage fullerenes; the higher LUMO levels (with more cathodic shifts) of the open-cage fullerene derivatives correspond to higher values of V_{oc} in the fabricated devices. [5]

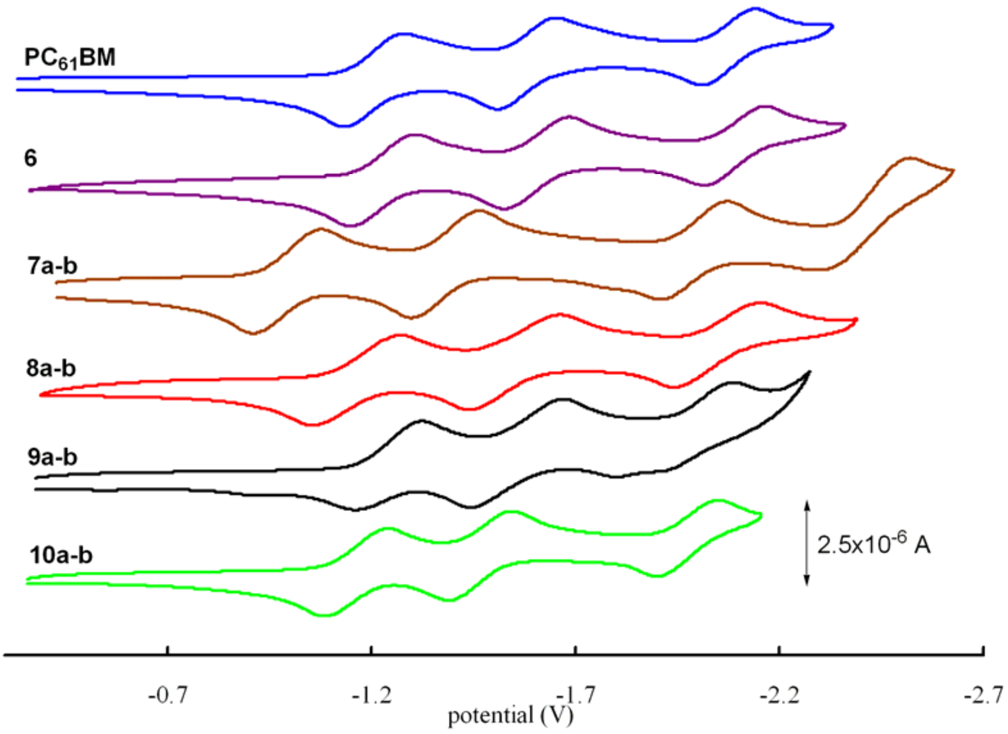

Figure 2. CV traces of **PC$_{61}$BM**, **6**, **7a-b**, **8a-b**, **9a-b**, **10a-b** in anhydrous *o*-DCB. Scanning rate: 50 mVs^{-1}.

These open-caeg fullerenes display interesting photovoltaics properties. We fabricated photovoltaic cells by spin-coating the blends of open-cage fullerenes and P3HT in *o*-DCB solution with layering configuration of glass/ITO/PEDOT:PSS/P3HT:open-cage fullerenes/Ca/Al using known protocols.[9] Table 3 summarizes the performances of the OPV devices incorporating **PC$_{61}$BM**, **6**, **7a-b**, **8a-b**, **9a-b**, **10a-b** and P3HT (see Fig. 3 for *J-V* plots). Their PCEs are all above 1.1% and not well correlated with their cage sizes. The observed relative order of V_{oc} values, **9a-b** > **6 > 10a-b** > **8a-b** > **7a-b,** are correlated with their LUMO energy levels, excepting for the relative order of **8a-b** and **10a-b**. To our delight, open-cage fullerene **6** exhibited the best and reproducible performance value of 2.9% among the open-cage compounds with P3HT (*ca.*10% less than that of a standard cell with

$PC_{61}BM$/P3HT recorded at the same condition; entries 1–2), with typical V_{oc} of 0.62 V, J_{sc} of 7.2 $mAcm^{-2}$, and FF of 66.0%. As expected, compound **7a-b** displayed lower efficiency at 1.3% with lowest V_{oc} of 0.40 V among all compounds due to its low LUMO energy level (entry 3). Upon raising 0.20 eV of the LUMO energy level through insertion of a sulfur atom in the rim of **7a-b** to give **8a-b**, PCE was improved about 0.5% with an increment of V_{oc} of 0.11 V (entry 4). We found that the performances of these open-cage fullerenes were also not consistent with their relative order of LUMO energy levels. Despite of its higher LUMO energy levels, the device performance shown by **9a-b**/P3HT is dissatisfying since compound **9a-b** tends to form precipitates in *o*-DCB solution during film formation, likely due to intermolecular hydrogen bonding through N-H. Its best performance of 1.6% was recorded with a concentration of 10 $mgmL^{-1}$ of **9a-b** for establishing a reasonable device (entry 5). It is noteworthy that the largest cage compound **10a-b** showed the worst performance with P3HT (entry 6), which is likely due to the higher extent of the ruptured π-structure that reduces the charge transport potential.[8d]

Table 3. *J-V* characteristics of devices incorporating **$PC_{61}BM$**, **6**, **7a-b**, **8a-b**, **9a-b** and **10a-b**.and P3HT (1:1, w/w).[a]

entry	compound	J_{sc}[b]	V_{oc} (V)	FF	PCE (%)	μ_e[c]
1	**$PC_{61}BM$**	7.4	0.65	0.66	3.2	6.0×10^{-8}
2	**6**	7.2	0.62	0.66	2.9	4.6×10^{-8}
3	**7a-b**	5.3	0.40	0.62	1.3	1.9×10^{-8}
4	**8a-b**	5.8	0.51	0.62	1.8	1.8×10^{-8}
5	**9a-b**[d]	4.9	0.65	0.51	1.6	1.4×10^{-8}
6	**10a-b**[e]	3.4	0.57	0.56	1.1	8.7×10^{-9}

[a] Data collected with concentration at 15 $mgmL^{-1}$ in *o*-DCB and film spin coated at 800 rpm unless otherwise noted. [b] Current density ($mAcm^{-2}$). [c] Units in $m^2V^{-1}s^{-1}$; values are determined from SCLC method. [d] Concentration of **9a-b** in 10 $mgmL^{-1}$. [e] Film spin coated at 1200 rpm.

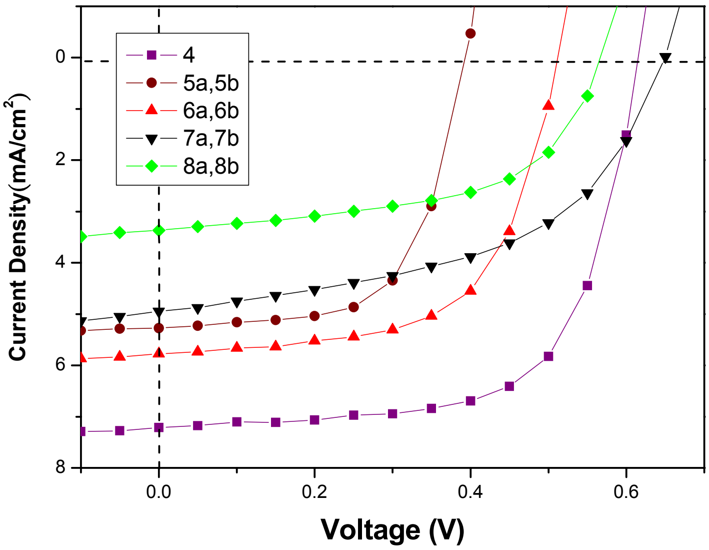

Figure 3. *J–V* curves of **6**, **7a-b**, **8a-b**, **9a-b**, **10a-b** and P3HT OPV devices.

We used the prepared open-cage fullerenes **8a-b** to attempt insertion of hydrogen at high pressure in an autoclave. We achieved insertion of hydrogen to obtain compound H_2@**8a-b** and insertion of ammonia to obtain NH_3@**10a-b**. The relatively large open fullerene **10a-b** can encapsulate a molecule of H_2O inside the cage spontaneously. We are preparing to publish these results in the near future. However, the attempt of inserting metallic species as gadolinium remains unsuccessful (Scheme 2). The insertion of a metallic species may need further modification of the rim of the open-cage fullerenes.

Conclusion

We have achieved to use metal-catalyzed reaction to obtain functionalization of fullerene C_{60}. We also obtain insertion of hydrogen, ammonia and water molecule inside the open fullerene cage; however, insertion of metallic species remains unsuccessful. In the future, we will explore application of these novel structures as n-type materials for organic solar cells.

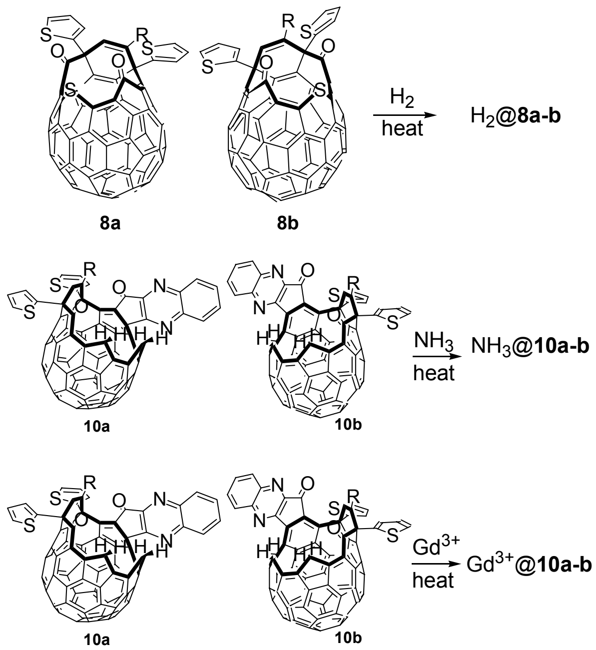

Scheme 2. Insertion of H_2 and NH_3 in **8a-b** and attempts of inserting Gd^{3+}.

參考文獻

---

[1] (a) Shabashov, D.; Molina Maldonado, J. R.; Daugulis, O. *J. Org. Chem.* **2008**, *73*, 7818–7821. (b) Daugulis, O.; Zaitsev, V. G. *Angew. Chem., Int. Ed.* **2005**, *44*, 4046–4048.

[2] Thirunavukkarasu, V. S.; Parthasarathy, K.; Cheng, C. H. *Angew.Chem. Int. Ed.* **2008**, *47*, 9462–9465.

[3] Kalyani, D.; Deprez, N. R.; Desai, L. V.; Sanford, M. S. *J. Am. Chem. Soc.* **2005**, *127*, 7330–7331.

[4] Inamoto, K.; Saito, T.; Katsuno, M.; Sakamoto, T.; Hiroya, K. *Org. Lett.* **2007**, *9*, 2931–2934.

[5] Chen, X.; Li, J. J.; Hao, X. S.; Goodhue, C. E.; Yu, J. Q. *J. Am. Chem. Soc.* **2006**, *128*, 78–79.

[6] Compound **10a** and **10b** each encapsulates a water molecule inside the cage in 79% and 54% ratio by ^{1}H NMR analyses, in which encapsulated H_2O appear at –11.28 and –11.34 ppm, respectively.

[7] Compound **7a-b**, **8a-b**, **9a-b** and **10a-b** are isolated as isomeric mixtures since they are difficult to be separated by flash column chromatography in low polarity solvents (toluene/hexanes = 1:1). Later, we find that their solubilities are even lower upon separated from their isomeric mixtures with Buckyprep column by HPLC. Our preliminary results show that these separated isomers give lower PCEs.

[8] (a) Murata, Y.; Murata, M.; Komatsu, K. *Chem. Eur. J.* **2003**, *9*, 1600. (b) Iwamatsu, S.-I.; Ono, F.; Murata, S. *Chem. Commun.,* 2003, 1269. (c) Iwamatsu, S.; Uozaki, T.; Kobayashi, K.; Re, S.; Nagase, S.; Murata, S. *J. Am. Chem. Soc.* **2004**, *126*, 2668.

[9] P3HT:open-cage fullerenes (15 mgmL^{-1}, 1:1 w/w) except for **7a-b** using 10 mgmL^{-1}. (a) Chen, C.-P.; Chan, S.-H.; Chao, T.-C.; Ting, C.; Ko, B.-T. *J. Am. Chem. Soc.*, **2008**, *130*, 12828. (b) Yu, C.-Y.; Chen, C.-P.; Chan, S.-H.; Hwang, G.-W.; Ting, C. *Chem. Mater.*, **2009**, *21*, 3262. (c) Chan, S.-H.; Hsiao, Y.-S.; Hung, L.-I.; Hwang, G.-W.; Chen, H.-L.; Ting, C.; Chen, C.-P. *Macromolecules.*, **2010**, *43*, 3399.